

## MINIREVIEW

View Article Online  
View Journal | View IssueCite this: *Nanoscale*, 2024, **16**, 4529

# Biomolecules meet organic frameworks: from synthesis strategies to diverse applications

Jing Li,<sup>a</sup> Chunyan Li,<sup>a</sup> Zelong Zhao,<sup>a</sup> Yuxue Guo,<sup>a</sup> Hongli Chen,<sup>b</sup> Pai Liu,<sup>a</sup> Meiting Zhao<sup>ID</sup>\*<sup>c</sup> and Jun Guo<sup>ID</sup>\*<sup>a</sup>

Biomolecules are essential in pharmaceuticals, biocatalysts, biomaterials, etc., but unfortunately they are extremely susceptible to extraneous conditions. When biomolecules meet porous organic frameworks, significantly improved thermal, chemical, and mechanical stabilities are not only acquired for raw biomolecules, but also molecule sieving, substrate enrichment, chirality property, and other functionalities are additionally introduced for application expansions. In addition, the intriguing synergistic effect stemming from elaborate and concerted interactions between biomolecules and frameworks can further enhance application performances. In this paper, the synthesis strategies of the so-called bio-organic frameworks (BOFs) in recent years are systematically reviewed and classified. Additionally, their broad applications in biomedicine, catalysis, separation, sensing, and imaging are introduced and discussed. Before ending, the current challenges and prospects in the future for this infancy-stage but significant research field are also provided. We hope that this review will offer a concise but comprehensive vision of designing and constructing multifunctional BOF materials as well as their full explorations in various fields.

Received 3rd November 2023,  
Accepted 28th December 2023

DOI: 10.1039/d3nr05586h

rsc.li/nanoscale

<sup>a</sup>State Key Laboratory of Separation Membrane and Membrane Process, School of Materials Science and Engineering & School of Chemistry, Tiangong University, Tianjin 300387, China. E-mail: junguo@tiangong.edu.cn

<sup>b</sup>Tianjin Key Laboratory of Optoelectronic Detection Technology and Systems, Tiangong University, Tianjin 300387, China

<sup>c</sup>Tianjin Key Laboratory of Molecular Optoelectronic Sciences, Department of Chemistry, Institute of Molecular Aggregation Science, Tianjin University, Tianjin 300072, China. E-mail: mtzhao@tju.edu.cn



Jun Guo

*Jun Guo received his BS degree from Huazhong University of Science and Technology in 2012. Then, he obtained his Ph.D. degree from Peking University and National Center for Nanoscience and Technology in 2018, under the guidance of Prof. Zhiyong Tang and Prof. Hailin Peng. In 2021, after finishing his postdoctoral career in Prof. Hua Zhang's group at City University of Hong Kong, he joined Tiangong University as a*

*full professor. Currently, his research interests mainly focus on the synthesis of multifunctional chiral nanomaterials for applications in catalysis, separation and biomaterials.*

## 1 Introduction

Biomolecules are essential components of living organisms and play a crucial role in sustaining basic life activities, including carbohydrates, proteins, nucleic acids, etc.<sup>1,2</sup> In addition to basic biological functions, biomolecules are also widely used in food production, drug synthesis, fine chemical industry, equipment manufacturing and other fields.<sup>3–5</sup> For example, the global enzyme market has increased significantly, reaching \$8.9 billion in 2021 and being estimated to reach up to \$13.25 billion by 2025.<sup>6</sup> Similarly, the recombinant DNA market in the global medical industry has shown substantial growth, valued at \$348.7 billion in 2022 and expected to reach \$500 billion by 2027.<sup>7</sup> Despite the significant advances, the susceptibility of biomolecules against extraneous conditions, such as nonaqueous solvents, high temperatures, strong acids or bases, and mechanical stress, causes a grand challenge to their practical use and further expansion.<sup>8–11</sup>

Porous organic framework materials, containing metal-organic frameworks (MOFs), hydrogen-bonded organic frameworks (HOFs), hydrogen-bonded inorganic-organic frameworks (HOIFs) and covalent organic frameworks (COFs), have become promising materials in various application fields.<sup>12–15</sup> Their inherent properties such as high surface areas as well as porosities, adjustable structures, and easily modifiable properties make them excellent platforms for biomolecule immobilization and installation.<sup>16–19</sup> Generally, three main

approaches can be adopted to integrate biomolecules with these frameworks to construct bio-organic frameworks (BOFs). These are: (1) attachment of biomolecules onto the external surface of pre-synthesized frameworks, (2) incorporation of biomolecules within the matrix of frameworks, and (3) utilization of biomolecules as building blocks for direct construction of novel frameworks.<sup>20–24</sup> The resulting BOFs are expected to not only significantly improve the thermal, chemical and mechanical stability of raw biomolecules but also introduce additional sieving, enrichment, chirality and other functions from the frameworks.<sup>25,26</sup> One elegant example reported by Chen *et al.*<sup>27</sup> presented a novel type of bifunctional WGL@NKCOF-118(M) [TAPP-PBMB; (TAPP = tetra-(4-amino-phenyl)porphyrin, PBMB = 4,4'-(1,4-phenylenebis-(ethyne-2,1-diyl))-bis-(2-methoxybenzaldehyde))] *via* integrating enzymatic wheat germ lipase (WGL) within the mesopores of photoactive porphyrinic NKCOF-118(M) (M = H, Zn, Cu, and Ni). The composited BOF exhibited good photocatalytic conversion efficiency, high product enantioselectivity and robust recyclability for asymmetric Mannich reactions.

Unexpected synergistic effects for further performance enhancement can be harnessed *via* elaborate interaction modulations. For example, cytochrome c (Cyt c) in which the heme ferric center adopts the low-spin hexa-coordination is a highly stable hemeprotein for electron transport in mitochondria.<sup>28</sup> Once carefully installed, the outer organic framework shell can not only retain the bioactivity of Cyt c even under harsh extracorporeal conditions but also contribute to performance improvement and even additional functionality. An elegant example was reported by Chen *et al.*,<sup>29</sup> who used NU-1000 [Zr<sub>6</sub>O<sub>4</sub>(OH)<sub>8</sub>TBAPy<sub>2</sub>] to encapsulate Cyt c for catalytic evaluations. The encapsulation of Cyt c inside NU-1000 resulted in a significant change in the coordination environment of the heme active site of raw Cyt c, which promotes the accessibility of the H<sub>2</sub>O<sub>2</sub> substrate to the catalytic heme site, thus boosting the reaction rate of catalyzing the ABTS oxidation compared to raw Cyt c.

Research studies based on BOFs have made tremendous progress recently and hold great promise for applications in biomedicine, catalysis, separation, sensing, and imaging.<sup>30–36</sup> Nevertheless, reviews introducing the combination of biomolecules with organic frameworks are not common in the existing literature, let alone a comprehensive summary involving biomolecules with all kinds of framework materials including MOFs, COFs and HOFs. Bearing these in mind, we comprehensively surveyed and summarized recent advances in the construction strategies of BOFs first. The broad applications of BOFs together with their improved performances in biomedicine, catalysis, separation, sensing and imaging are then introduced and discussed. Before ending, we further provide our personal opinions on the current challenges of BOFs and future research directions in this infancy research area. It is hoped that this review can provide fast guidance for the rational design and sophisticated construction of multifunctional BOF materials as well as their full exploration in various application fields.

## 2 Synthesis strategies of BOFs

### 2.1 Attachment of biomolecules onto frameworks

Biomolecules such as amino acids, proteins, polysaccharides, *etc.* that feature abundant binding sites can be directly attached onto the surface of prefabricated MOFs<sup>37–39</sup> COFs<sup>40–42</sup> and HOFs<sup>43–45</sup> through covalent bonding, coulombic attractions,  $\pi$ - $\pi$  stacking, hydrogen bonding, and intermolecular force. Chen *et al.*<sup>39</sup> reported an example of the modification of a tumor-homing F3 peptide onto surfaces of doxorubicin (DOX)-encapsulated MOFs by covalent linkage (Fig. 1A). The intrinsically radioactive <sup>89</sup>Zr-UiO-66 [Zr<sub>6</sub>O<sub>4</sub>(OH)<sub>4</sub>BDC<sub>12</sub>] was elaborately selected as the platform for the construction of the multifunctional BOF material. First, <sup>89</sup>Zr-UiO-66 of positron emission tomography (PET) imaging capability was grafted with pyrene-derived poly(ethylene glycol). Then, it can be surface-engineered to incorporate targeting ligands, such as the F3 peptide targeting nucleolin with the purpose of specific targeting to tumor cells.

COFs, composed of light organic elements, are more bio-compatible and less toxic than MOFs but usually lack good targeting ability as biological platforms.<sup>27,33</sup> A smart strategy for exosome-targeted DNA functionalization of COFs was reported by Lu *et al.*<sup>41</sup> To be specific, alkynyl-modified COFs were pre-synthesized with 1,3,5-tris(4-aminophenyl) benzene (TPB) and 2,5-bis(2-propynyloxy) terephthalaldehyde (BPTA) firstly. Then a Cu(I)-catalyzed azide/alkynyl cycloaddition reaction was used to functionalize azide-DNA on alkynyl-COFs (Fig. 1B). The bio-sensor constructed with DNA-COFs can identify exosomes specifically through the hybridization of cholesterol-tagged DNA, as well as detect and quantify exosomes with high sensi-



**Fig. 1** (A) Synthesis of <sup>89</sup>Zr-UiO-66/Py-PGA-PEG-F3. Reproduced with permission from ref. 39. Copyright 2017 American Chemical Society. (B) Synthesis of DNA-COFs. Reproduced with permission from ref. 41. Copyright 2022 American Chemical Society. (C) Synthesis of 2D-HOF and the hybrid membrane. Reproduced with permission from ref. 43. Copyright 2018 Wiley.

tivity. Moreover, Huang *et al.*<sup>42</sup> adopted a peptide-based surface modification to enhance the specific recognition of COFs towards transferrin (Tf). After modification of T10 (a Tf-binding ligand) peptide with high affinity, a hollow COF was endowed with a homing ability to deliver glioma drugs, thereby overcoming the grand challenge of the concealed location of gliomas in the central nervous system impeded by blood-brain barriers. Other biomolecules have also been selected for the surface functionalization of COFs.<sup>40,41,76</sup>

In contrast to harsh environments such as high pressure, high temperature or strong acidity typically involved in the syntheses of MOFs and COFs, the emerging HOFs consisting of dynamic hydrogen bonding enable a more gentle crystallization process. This makes the biomaterials based on HOFs have better compatibility with introduced biomolecules. As shown in Fig. 1C, Ye *et al.*<sup>43</sup> prepared multifunctional CS/PVA/LPB/HOF by surface cross-linking chitosan (CS) and 2D-HOF (MA-PMDA), using polyvinyl alcohol (PVA) and lauramide propyl betaine (LPB) as binders. Among the composite, the 2D-HOF was synthesized using a simple isothermal method. The binding process with the biomolecules and other constituents was also carried out under mild conditions. Impressively, the 2D-HOF improved biocompatibility and overall toughness, while natural CS resulted in antimicrobial properties and good bio-adhesion.

## 2.2 Encapsulation of biomolecules inside frameworks

The easy leaching and inactivation of surface-immobilized BOF types heavily constrained and even hindered their further applications in practice due to the weak interaction between the biomolecules and the pre-synthesized organic frameworks.<sup>46,47</sup>

Fortunately, the strategy of biomolecule encapsulation has well-resolved this issue. On the one hand, the active biomolecule is well separated within the matrix of frameworks free of escape and aggregation. On the other hand, the full shield of a highly porous shell further guarantees the innate activities of the biomolecules without environmental influences. Until now, there were many examples of biomolecule encapsulation that can be normally sorted as post-modification and *in situ* installation protocols.<sup>48–51</sup> For instance, Chen *et al.*<sup>30</sup> reported the encapsulation of Cyt c within mesoporous NU-1000 [ $\text{Zr}_6\text{O}_4(\text{OH})_4\text{BDC}_{12}$ ] and further assessed the catalytic activity of Cyt c@NU-1000 in oxidation applications. Upon encapsulation, the Cyt c conformation around the active center differed and led to enhanced performance in catalyzing the oxidation of ABTS rather than free Cyt c. Nevertheless, this post-corking approach was usually impeded by the limited pore size of most framework materials. Instead, Ouyang *et al.*<sup>52</sup> reported an *in situ* strategy by mimicking the biomineralization in which functional groups such as carboxylates and amines can promote framework formation around biomolecules. As shown in Fig. 2A, the strong coulombic charge interaction between carboxylates and metal ions accelerated the formation of BOFs around HRP. This study also demonstrated that  $\gamma$ -poly-L-glutamic acid (PGLA) peptide modulators can regulate the resultant nanostructure and pore size. Previously, the most extensively studied enzyme@3D micropore ZIF-8 [ $\text{Zn}(\text{min})_2$ ] that did not contain PLGA modulators retained only 0.6% of its raw activity.<sup>53,54</sup>

Yu *et al.*<sup>55</sup> proposed a synthetic method for promoting the entrance of biomolecules into pores of organic frameworks using a biomimetic mineralization strategy (Fig. 2B). Specifically, biocompatible HOFs [(1,4-benzenedicarboximida-



**Fig. 2** (A) Synthesis of deformable MOFs modulated by PLGA. Reproduced with permission from ref. 52. Copyright 2020 Wiley. (B) Synthesis of NSC@PCN/HOF. Reproduced with permission from ref. 55. Copyright 2022 Wiley. (C) Synthesis of enzyme@ZIF-8. Reproduced with permission from ref. 58. Copyright 2022 Elsevier.



mide)2-TBA<sub>4</sub>] were used for the encapsulation of neural stem cells (NSCs) through electrostatic interactions and hydrogen bonds between the HOFs and protein residues on the cell membranes. Furthermore, porous carbon nanospheres (PCNs) are intermixed in the HOF shells when being mineralized. Thanks to the antioxidant functionality of PCNs, the survivability of NSCs can be enhanced after encapsulation. During the past decade, the damage homing, differentiation and regenerative capacity of stem cells has attracted great attention in regenerative medicine and disease treatment. Nevertheless, the rate of cell delivery restricted the treatment of NSC transplantation.<sup>56,57</sup> Compared to conventional materials, biocompatible BOFs could overcome the common issues of poor treatment outcomes during NSC transplantation and therefore confer better survival of NSCs.

Unlike the biomolecule-induced defect generation during the synthesis of the BOFs mentioned previously, Feng *et al.*<sup>58</sup> introduced defect in enzyme-embedded MOFs (Fig. 2C) for the installation of biomolecules. Specifically, 2-methylimidazole partially replaced with 1-methylimidazole during the formation of ZIF-8 and resulted in defective ZIF-8 (d-ZIF-8). Impressively, the mesopores arising from defects could enhance the encapsulation and transportation of enzyme substrates. The researchers also demonstrated that the glucose oxidase (GOx) enveloped in the defective MOFs showed higher activity than GOx in normal MOFs.

### 2.3 Utilization of biomolecules as framework backbones

Biomolecules usually have reactive functional groups involving carboxyl, amino, and hydroxyl groups, allowing them to be used as building blocks for the direct synthesis of BOFs.<sup>22,25</sup> It is commendable to obtain better biocompatibility by using a

more direct synthesis strategy than the others described above. Amino acids have rich carboxyl and amino groups and therefore are considered ideal linkers for the construction of biological MOFs.<sup>81</sup> Specifically, Wang *et al.*<sup>59</sup> synthesized a MIP-202(Zr) [Zr<sub>6</sub>O<sub>4</sub>(OH)<sub>4</sub>(L-aspartic acid)<sub>12</sub>] using aspartic acid directly as the ligand, in which, the classical 12-coordinated Zr<sub>6</sub>(μ<sub>3</sub>O)<sub>4</sub>(μ<sub>3</sub>-OH)<sub>4</sub> nodes and dicarboxylic L-aspartic acid were reacted under hydrothermal conditions to generate a 3D microporous net (Fig. 3A). Thanks to strong coordination between zirconium(IV) and carboxylate, assembled biological MIP-202(Zr) exhibited good chemical stability under various conditions including a wide pH range of aqueous solutions, boiling water and conventional organic solvents.

In some cases, BOFs with well-defined crystal and typical pore structures are hard to directly synthesize from asymmetric and flexible amino acids. To conduct more successful syntheses, it is necessary to modify raw amino acids with rigid skeletons and/or additional coordination sites. As shown in Fig. 3B, the aspartic acid-modified ligand was reacted with Cu<sup>2+</sup> and Ca<sup>2+</sup> ions, where the carboxylate group of the aspartic acid part is bridged to the Cu<sup>2+</sup>.<sup>60</sup> The coordination of amino acids with Ca<sup>2+</sup> is mediated by water molecules, forming multiple hydrogen-bonded interactions among the [Ca<sub>3</sub>(μ-H<sub>2</sub>O)<sub>4</sub>(H<sub>2</sub>O)<sub>17</sub>]<sup>6+</sup> clusters and finally constituting a stable and huge hydrated calcium environment.

The multiple potential coordination sites of nucleobases and their rigid structures make them also suitable for the synthesis of biological MOFs with the assistance of metal ions. As two common types of nucleobases (*i.e.* purines and pyrimidines), the unique purine nucleobase consists of four heterocyclic N atoms and one outer ring amino N atom, which can be combined with metals *via* a variety of binding modes. For



**Fig. 3** (A) Structure of MIP-202(Zr). Reproduced with permission from ref. 59. (B) Structure of Cu<sub>10</sub> cages. Reproduced with permission from ref. 60. Copyright 2021 American Chemical Society. (C) Structure of bio-MOF-11. Reproduced with permission from ref. 61. Copyright 2020 American Chemical Society. (D) Structure of SION-19. Reproduced with permission from ref. 62.

example, bio-MOF-11  $[\text{Co}_2(\text{adenine})_2(\text{CH}_3\text{CO}_2)_2]^{61}$  was synthesized by using both acetic acid and pyrimidines as ligands (Fig. 3C). Moreover, Anderson *et al.*<sup>62</sup> reported a BOF  $[\text{Zn}_6\text{O}(\text{adenine})\text{TBAPy}_2]$  composed of pyrimidine with a larger molecule [1,3,6,8-tetra(*p*-benzoate) pyrene]. This BOF had a fluent Watson–Crick<sup>95</sup> surface pointing to the cavity of adenine (Ade) (Fig. 3D), and a large pore channel embraced by 1,3,6,8-tetra(*p*-benzoate) and thymine. Noteworthy, this approach of using BOFs as nanoreactors to connect biologically relevant molecules can bridge multiple research disciplines and help develop new bioplatfroms for drug discovery and delivery.

Except for small molecules, macromolecular peptides, proteins and polysaccharides are also feasible for the construction of BOFs in various forms. There are not many examples of direct synthesis of BOFs from peptides, and the longest peptide ligand reported is a tripeptide, to the best of our knowledge. Sorrenti *et al.*<sup>63</sup> reported novel BOF single crystals formed by a coordinated assembly of  $\text{Cu}^{2+}$  with tripeptide glycine–histidine–glycine (Fig. 4A). To gain morphological control during biomineralization, crystal growth was limited in microfluidic environments mimicking microgravity conditions. A physical model of the reactive diffusion theory was also established, which revealed that the final growth speed strongly relied on the diffusion rate from the solution to the crystal surface. The ability to grow megascopic single crystals with adaptable pores as well as controlled size and shape allows for the optimization of their properties and further expands their application scopes.

Based on the dehydration of multiple amino acids to form peptide bonds, many peptides are folded together to form protein molecules. As shown in Fig. 4B, the first example of a 3D protein-MOF  $[\text{Zn}^{\text{T122H}}\text{ferritin}]$  was reported by Sontz *et al.*<sup>64</sup> Unlike previous lattice structures of MOFs depending on the metal nodes and organic pillars, the researchers

created a system using symmetrical proteins (highly stable human heavy chain ferritins) as the so-called metal nodes. The researchers engineered the octahedral enzyme ferritin with tripod zinc coordination in its C3 symmetrical wells. The presence of  $\text{Zn}^{2+}$  triggered the self-assembly of the Zn-ferritin into the desired bcc-type bio-framework crystals upon coordination of a ditopic linker bearing hydroxamic acid functional groups. This work represented the first example of a protein–metal–organic framework.

Natural proteins normally need to bind metal ions at specific sites to ensure suitable protein folding. However, it is hard to manage the coordination of metal ions on protein surface due to their high complexity and flexibility.<sup>65</sup> Therefore, there are still few examples of protein–metal ion coordination for the synthesis of BOFs so far. The problem of synthesis due to protein folding is well resolved in the BOF formed by the self-assembly of proteins *via* hydrogen bonds, which was reported by Chen *et al.*<sup>66</sup> In this case, the N–H and COOH residues in the protein provided rich hydrogen bond sites, which drove the assembly to form a highly crystalline hybrid framework. Since amino acid residues are commonly found in proteins, it is also feasible to use this assembly method to construct BOFs consisting of other proteins such as Cyt c, ovalbumin (OVA), and transferrin (TRF).

In addition to the above biomolecules, polysaccharide-based organic frameworks have awakened great research interests due to their biocompatibility and structural strength among the various BOFs.<sup>67,68</sup> Polysaccharides with relatively rigid ring structures not only guaranteed the mechanical strength but also made resultant organic framework permeant porosity.<sup>69,70</sup> Among them, BOFs based on cyclodextrins (CD) are the most widely used polysaccharide-BOFs because of their inherent cavities (17 Å generated by CD) and the existence of a lot of hydroxyl groups.<sup>71</sup> These make them promising candi-



**Fig. 4** (A) Synthesis of CuGHG. Reproduced with permission from ref. 63. Copyright 2020 American Chemical Society. (B) Synthesis of  $\text{Zn}^{\text{T122H}}\text{ferritin}$ . Reproduced with permission from ref. 64. Copyright 2015 American Chemical Society. (C) Structure of  $(\gamma\text{-CD})_6$  units. Reproduced with permission from ref. 72. Copyright 2020 American Chemical Society.

dates for the adsorption and separation applications of diversified gases and other organic small molecules. In a latest research, Shen *et al.*<sup>72</sup> reported a method for the co-assembly of  $\gamma$ -cyclodextrin ( $\gamma$ -CD) and organic counterbalancing anions to form BOFs. In specification,  $\gamma$ -CD was used as the primary block and a 4-methoxysalicylic acid ( $4\text{-MS}^-$ ) anion was used as the auxiliary to form a novel type of BOF thorough coordination, and electrostatic and dispersion forces, in which,  $\gamma$ -CD was coordinated with the  $\text{K}^+$  ion and was further connected with the  $4\text{-MS}^-$  anion through hydrogen bonds. Fig. 4C shows the sectioned view of BOFs, the  $4\text{-MS}^-$  anion was involved in the construction of the hybridized framework and acted as a supramolecular baffle.

BOFs consisting of multiple kinds of biomolecules have also been reported. Lan *et al.*<sup>73</sup> reported a BOF constructed by integrating active metal centres, proximal amino acids and other modulators into a tunable MOF monolayer. An underlying monolayer MOF  $[\text{Hf}_{12}(\mu_3\text{-O})_8(\mu_3\text{-OH})_8(\mu_2\text{-OH})_6(\text{Ir-PS})_6(\text{TFA})_6]$  was constructed by an  $\text{Hf}_{12}$  cluster vertically capped by trifluoroacetate (TFA) and photosensitizing Ir (4,4'-di(4-benzoato)-2,2'-bipyridine) [2-(2,4-difluorophenyl)-5-(trifluoromethyl) pyridine]<sup>2+</sup> (Ir-PS) ligands firstly. By exchanging TFAs with more strongly coordinating carboxylate groups, the ferric protoporphyrin haemin and amino acids could be installed onto Hf-Ir to form BOFs. Through tuning the incorporated amino acids in the BOFs, the authors systematically optimize the activity and selectivity of these BOFs to perform photocatalytic  $\text{CO}_2$  reduction and water oxidation reactions. Guo *et al.*<sup>74</sup> reported a strategy that relies on accelerating the formation of BOFs around proteins *via* the self-assembly of protein/polyvinylpyrrolidone/cysteine. Notably, the highly encapsulated protein can maintain its natural structural conformation and the tightness of structural constraints within ZIF-8 confers excellent biological activity to the protein/enzyme even under harsh conditions of particular denaturation or inhibition of free enzyme. The feasibility of this bionic

strategy has also been demonstrated for biomedicine loading, enzyme cascades and biosensing.

Among the several methods described above for forming biological organic frameworks, the synthesis method of attaching biomolecules onto the surface of the organic framework is a simply and regularly used method.<sup>20</sup> However, the attachment method especially relying on electrostatic adsorption usually has the disadvantages of inhomogeneity and easy disruption. Hence, the improved method *via* covalent attachment is considered a more reliable one. The encapsulation method can protect biomolecules from aggregation and escape, and more importantly, addresses the denaturing of biomolecules. Meanwhile, the disadvantage of this method is also conspicuous, namely the narrow size constraint of encapsulated biomolecules. When biomolecules are directly used as ligands to form BOFs, there is no more need to prepare frameworks in advance and also no limitation for the biomolecular dimensions. Unfortunately, the successful examples reported until now were still rare.

### 3 Applications of BOFs

By combining the properties and characteristics of biomolecules and organic frameworks, BOFs have drawn intense interest in various fields. In particular, compared with MOFs and COFs, the better biocompatibility and biodegradability of BOFs make them the mainstream trend of modern biomaterials. In this part, we will introduce the remarkable achievement of BOFs in a wide range of applications ranging from biomedicine, catalysis, adsorption, separation, sensing, and imaging.

#### 3.1 BOFs for biological medicine

BOFs have proved to be a rising platform for drug delivery because of their high drug-loading ability, biodegradability and multifunctionality.<sup>75</sup> As shown in Fig. 5A, Zhang *et al.*<sup>76</sup>

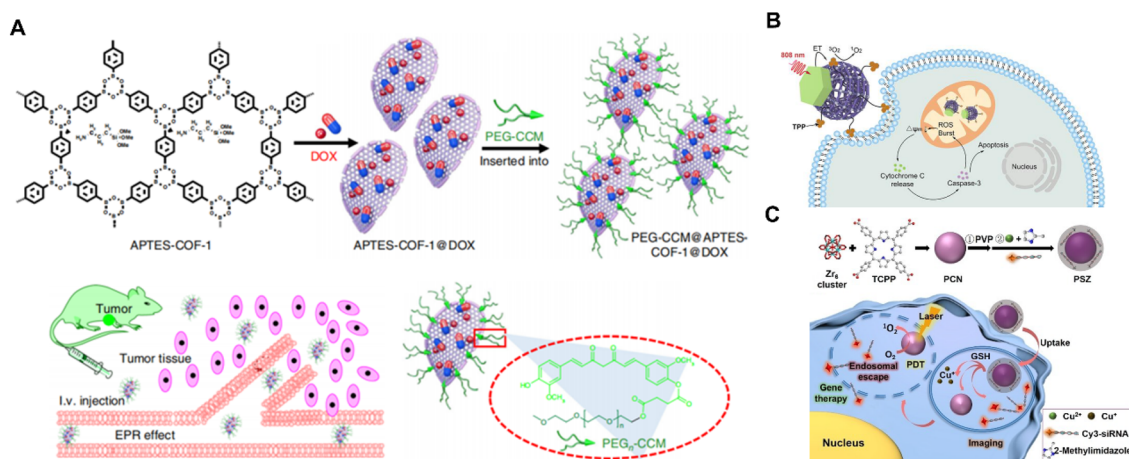


**Fig. 5** (A) Synthesis and drug delivery of PEG-CCM@APTES-COF-1@DOX. Reproduced with permission from ref. 76. (B) Schematic illustration of the upconversion MOFs for mitochondria-targeted PDT. Reproduced with permission from ref. 77. Copyright 2020 Wiley. (C) Synthesis of PSZ and the mechanism of enhanced PCN-mediated PDT with GSH depletion. Reproduced with permission from ref. 78. Copyright 2022 Wiley.



ation by cells and activation by GSH, the outer shell dissociated and released the siRNA for GSH imaging and subsequent gene silencing. At the same time, the photosensitizing core was unlocked for intensified PDT together with GSH depletion. The reported BOF overcame the GSH-associated resistance and provided a new approach for designing intracellular stimulus-activated theranostics.

Except for the aforementioned therapeutic approaches through pH response, other factors such as light and heat response are also commonly available for triggering drug release. Liu *et al.*<sup>77</sup> designed Nd<sup>3+</sup>-sensitized upconversion MOFs (UCMTs) as a mitochondria-targeted photodynamic therapy (PDT) platform induced by near-infrared (NIR) light (Fig. 5B). The UCMTs possessed a Janus nanostructure feature composed of Nd<sup>3+</sup>-sensitized upconversion nanoparticles and porphyrinic nMOFs (ZrOTCPP) with further surface functionalization of triphenylphosphine. Through effective resonance energy transfer (RET) of Nd<sup>3+</sup> sensitized upconversions to the nMOF domains, UCMT allows the generation of reactive oxygen species (ROS) under 808 near-infrared light activation. Furthermore, Liu *et al.*<sup>78</sup> reported a BOF for intelligent glutathione (GSH) imaging while simultaneously reducing GSH levels. The BOF consisted of a photoactive MOF as the core and susceptible ZIF-67(Cu) as the shell with the installation of additional cyanine 3-labeled siRNA. Upon internalization,

Enzymes are well-recognized as highly efficient and selective naturalistic catalysts. Nevertheless, the vulnerabilities of enzymes such as low thermal stability, narrow pH tolerance range and poor tolerance in organic solvents heavily hinder their further application.<sup>25</sup> Due to their large pore structures and tunable chemical properties, organic frameworks are suitable as hosts for immobilizing enzymes. Xia *et al.*<sup>79</sup> reported NH<sub>2</sub>-MIL-101 [Fe<sub>2</sub>(BDC)<sub>3</sub>-NH<sub>2</sub>] (designated as qNM) to immobilize enzymes with good oxidation catalytic activity (Fig. 6A). The qNM showed a good ability to oxidize different peroxidase substrates. The qNM can be further combined with GOx or both  $\beta$ -galactosidase ( $\beta$ -Gal) and GOx for a cascade reaction. The obtained catalytic activity was increased by 2.67-fold and 1.83-fold, respectively, in comparison with the corresponding free enzyme. More importantly, because of the strong covalent interactions, the immobilized enzyme exhibited increased stability in harsh chemical environments, providing opportunities for applications in practice.

Enzyme-based BOFs have gained wide applications in the catalytic conversion of CO<sub>2</sub>. In Fig. 6B, Chen *et al.*<sup>80</sup> used a MOF to stabilize formate dehydrogenase (FDH) in an acidic environment for the bio-electrocatalytic reduction of CO<sub>2</sub>. The

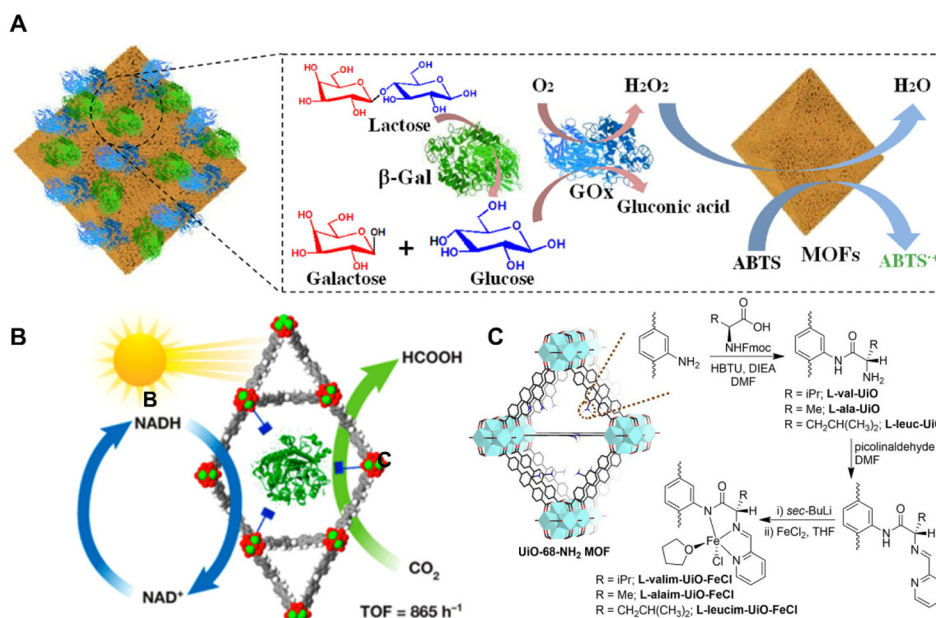


**Fig. 6** (A) Schematic illustration of  $\beta$ -Gal/GOx-qNM cascade reactions. Reproduced with permission from ref. 79. Copyright 2021, American Chemical Society. (B) Schematic diagram of a bio-electrocatalytic  $\text{CO}_2$  reduction reaction. Reproduced with permission from ref. 80. Copyright 2019 Wiley. (C) Synthesis of amino acid-derived UiO-68- $\text{NH}_2$  and metalation with  $\text{FeCl}_2$ . Reproduced with permission from ref. 81. Copyright 2021 Wiley.

researchers encapsulated FDH in NU-1006  $[\text{Zr}_6\text{O}_4(\text{OH})_4]_{4',4'',4''',4''''}$ -(pyrene-1,3,6,8-tetrayl)tetrakis(2',2'',5',5'''-tetramethyl-[1,1':4',1''-terphenyl]-4-carboxylic acid)<sub>12</sub>] to enhance its stability and catalytic activity. The hierarchical pore structure of NU-1006 not only allowed for the inclusion of the large-size enzyme but also facilitated substrate diffusion. After encapsulation, enhancement of the activity on producing nicotinamide adenine dinucleotide (NADH) from  $\text{NAD}^+$  was utilized for electrochemical conversion of  $\text{CO}_2$  into formic acid with high efficiency. This approach provided a simple and efficient method for  $\text{CO}_2$  fixation and showed great potential in the electroreduction of excess  $\text{CO}_2$  even from the atmosphere.

In addition to enzymes, amino acid-based BOFs have also shown applications in catalysis. Newar *et al.*<sup>81</sup> reported the highly active and enantioselective catalysts based on amino acid-functionalized MOFs in asymmetric organic transformations (Fig. 6C). The authors grafted amino acids within the pores of UiO-68- $\text{NH}_2$  MOF  $[\text{Zr}_6\text{O}_4(\text{OH})_4(\text{L-NH}_2)_6(\text{L-NH}_2 = 2'\text{-amino-[1,1':4',1''-terphenyl]-4,4''-dicarboxylate})]$  and further introduced catalytic iron sites *via* post-synthetic metalation. The catalysts prepared using this method exhibited excellent catalytic activity (>99%) and enantioselectivity (>99% ee) for 10 examples in the asymmetric reduction of ketones, which was significant for the sustainable synthesis of optically active compounds.

### 3.3 BOFs for adsorption and separation

BOFs are also emerging candidates for enantioselective adsorptions and chiral separations. In comparison with conventional MOFs and COFs, biomolecules are naturally chiral substances and therefore can be directly adopted to finely modify the chiral environment of BOFs, which endowed them with excellent enantioselectivity. It was reasonable to design BOFs as nanoarrays characteristic of periodic chiral channels for chiral substrate adsorption.<sup>96</sup> By adjusting and controlling the pore size, shape, and functional groups, high adsorption amounts and excellent enantioselectivity could be harnessed at the same time. Sánchez *et al.*<sup>82</sup> reported a chiral  $\text{Cu}(\text{II})$  3D MOF  $[\text{Cu}(\text{Gly-L-His-Gly})]$ , which was used to enantioselectively adsorb racemic methamphetamine and ephedrine (Fig. 7A). The authors conducted simulations, which implied that chiral discrimination was achieved because one of the enantiomers preferentially formed diastereomeric adducts with the frameworks in thermodynamics. The authors also demonstrated that further developed solid phase extraction (SPE) using  $[\text{Cu}(\text{Gly-L-His-Gly})]$  successfully isolated the enantiomers from a racemic mixture in only four minutes.

Chiral separation is also a vital approach for producing drugs and bioactive substances since enantiomers of the different handedness differ greatly in their biological behav-

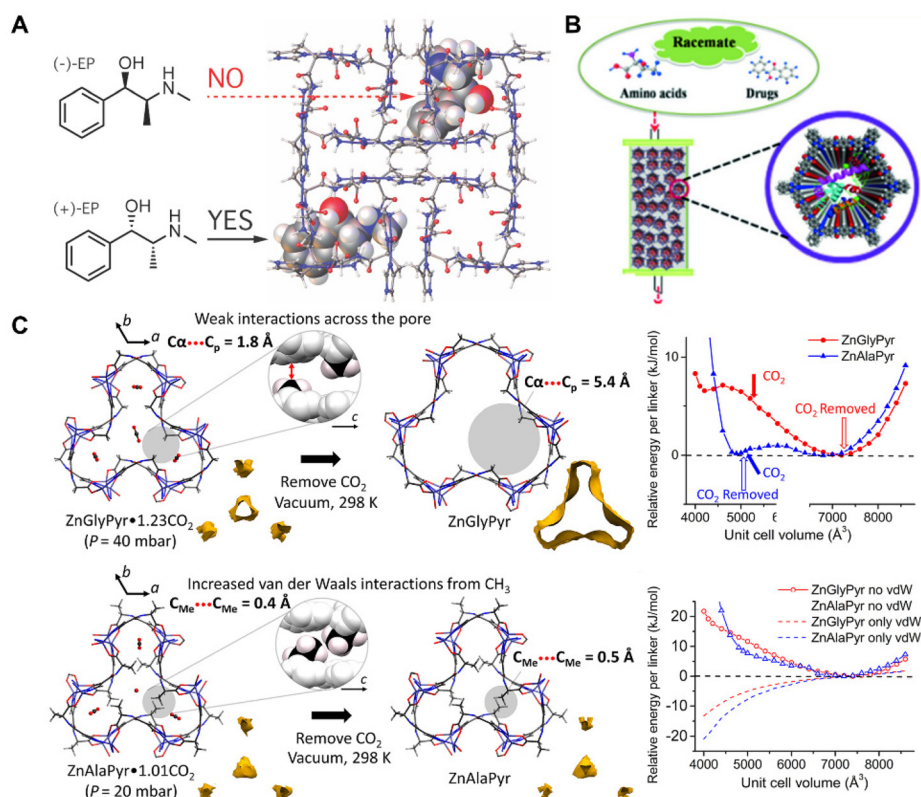


**Fig. 7** (A) Mechanism of Cu(GHG) for chiral recognition and discrimination. Reproduced with permission from ref. 82. Copyright 2017 American Chemical Society. (B) Illustration of lysozyme @ COF 1 based CSPs for chiral separation. Reproduced with permission from ref. 83. Copyright 2018 Wiley. (C) Mechanism of ZnXPyr  $\text{CO}_2$  removal and calculated  $E-V$  curves. Reproduced with permission from ref. 84.



our, metabolism, and toxicity. Zhang *et al.*<sup>83</sup> reported biomolecules C COFs of efficient chiral resolution ability by covalently modifying various biomolecules into achiral COF (Fig. 7B). Compared to the traditional modified methods, the proposed strategy renders COF composites ideal materials for the preparation of highly efficient and durable chiral stationary phases because of their high loading amounts and slow leakage rates. The BOF has been used in a variety of separation modes including both positive and inverse phases, which successfully separated various chiral substrates such as amino acids and chiral drugs at separation degrees above 1.3. After 2 months of continuous usage and more than 120 repeated samples, the resultant BOF still had the same separation effect as the initial state, demonstrating excellent reuse and reproducibility.

Apart from chirality-related applications, some BOFs even showed unique advantages in the capture of carbon dioxide to avoid devastating climate changes. Compared with conventional MOFs and COFs, the introduction of specific biomolecules can accurately adjust the pore microenvironment for intimately confining carbon dioxide. Yan *et al.*<sup>84</sup> reported a family of flexible MOFs [ZnX(Pyr), X = glycine or alanine, Pyr = pyrazole] based on derived amino acid ligands (Fig. 7C). The pyrazole and carboxylic acid groups were both coordinated to Zn(II) ions in a tetrahedral mode to form infinite [ZnX(Pyr)]<sub>∞</sub> helical rods. Each [ZnX(Pyr)]<sub>∞</sub> helical rod was further connected to a honeycomb net with a dynamic pore environment *via* the NH...OCH bonding. Impressively, ZnAlaPyr and ZnGlyPyr exhibited distinct adsorption and desorption isotherms towards CO<sub>2</sub>. Particularly at similar CO<sub>2</sub> uptakes, the second

step of CO<sub>2</sub> adsorption differed greatly accompanied by distinct adsorbed conformations between two frameworks.

### 3.4 BOFs for imaging and sensing

BOFs can be readily applied in the sensing and imaging fields, including computed tomography,<sup>85</sup> optical imaging or magnetic resonance imaging.<sup>86</sup> For instance, Mao *et al.*<sup>87</sup> described an effective biosystem for biosensing applications, which consisted of MOF-based nanozymes and G-quadruplex (G4)-DNAs. In specification, they linked MIL-53(Fe) [Fe<sub>3</sub>(OH)BDC, BDC = 1,4-benzenedicarboxylic acid] together with the G4 forming sequence (F3TC) through covalent bonding (Fig. 8A). Due to the resonated communication between F3TC and MIL-53(Fe), the obtained composite showed excellent peroxidase oxidative activity and good performance stability. The resultant BOF was further used as a biosensor for the detection of alkaline phosphatase (ALP) in human plasma samples with a quite low detection limit (LOD, 0.02 U L<sup>-1</sup>).

Dou *et al.*<sup>88</sup> reported a BOF consisting of a Zr-based MOF [ZrBCTPE<sub>2</sub>, BCTPE = 4'-(1,2-diphenylethene-1,2-diyl)dibenzoic acid] and Cy3-combined aptamer as a fluorescent sensor for aflatoxin B1 recognition (Fig. 8B). The nanoscale MOFs (NMOFs) were integrated with the aptasensor through electrostatic interaction between the positive charge on the surface of the NMOFs and the negatively charged AFB1 aptamer. This BOF-based aptasensor had the advantages of low complexity, output proportional signal, high specificity and stability, and had been applied in real corn samples. Efficient sensing and imaging of biomarkers is of great importance for clinical diagnosis and biomedicine. Messenger RNA (mRNA) has impor-

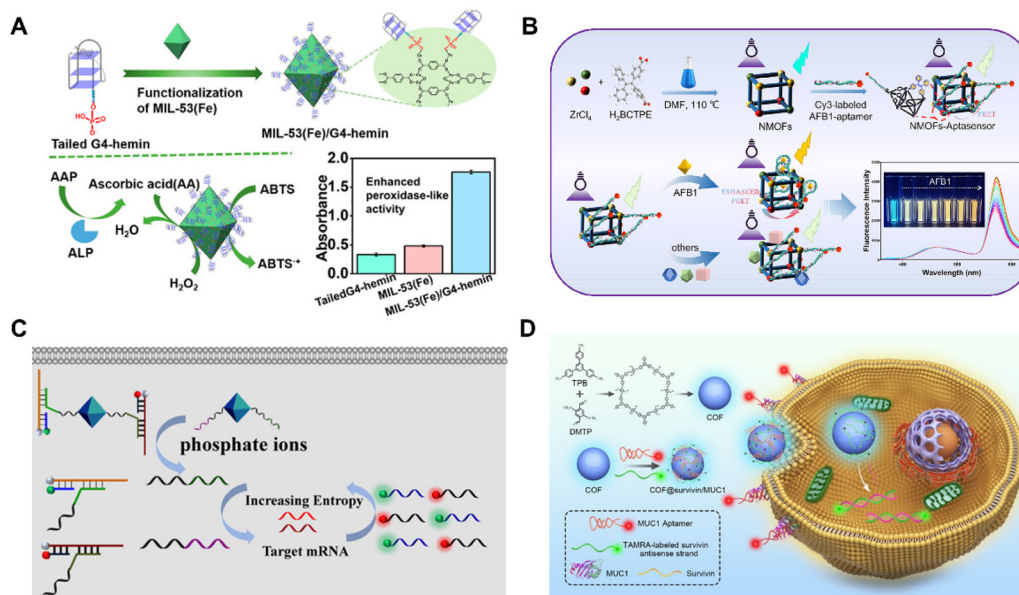


**Fig. 8** (A) Synthesis and the application in biosensing of the BOF. Reproduced with permission from ref. 87. Copyright 2022 American Chemical Society. (B) Synthesis and work process of the BOF-based sensor. Reproduced with permission from ref. 88. Copyright 2023 Elsevier. (C) Mechanism of DNA amplifier-MOF. Reproduced with permission from ref. 89. Copyright 2020 American Chemical Society. (D) Synthesis and the application in imaging of the BOF. Reproduced with permission from ref. 90. Copyright 2021 American Chemical Society.

tant biological functions in living systems and is a useful class of cancer biomarkers. As shown in Fig. 8C, Meng *et al.*<sup>89</sup> combined DNA with MOF nanoparticles to achieve multiple recognition and imaging of mRNA. This method utilized UiO-66 [ $\text{Zr}_6\text{O}_4(\text{OH})_4\text{BDC}_{12}$ , BDC = terephthalate] nanoparticles as carriers and functionalized DNA as amplifiers. Given that the UiO-66 nanoparticles had a small size and good stability, efficient penetration and uptake by cells were anticipated. Additionally, the large surface area of the UiO-66 nanoparticles provided abundant binding sites available for interacting with DNA amplifiers. This method successfully achieved the detection and imaging of intracellular mRNA in HepG2 cells. The high sensitivity of the DNA amplifier and the efficient MOF delivery system enabled the detection of low-abundance mRNA, providing a new method for early cancer diagnosis. The detection and imaging of intracellular mRNA could reveal dynamic changes in biological processes, providing a new tool for biological research. Additionally, the colourful organic chromophores of COFs also give them a broad-spectrum absorption ability to quench the fluorescence of various dyes. The combination of bio-molecules further endows the COFs with other biological activities.<sup>41</sup> For example, Gao *et al.*<sup>90</sup> developed a COF-based fluorescent nanoprobe (COF@survivin/MUC1) and applied it to simultaneously imaging biomarkers with different distributions in live cells (Fig. 8D). The nano-scale fluorescent COF (TPB-DMTP) could adsorb Cy5-tagged transmembrane glycoprotein mucin (MUC1) aptamer and the TAMRA-tagged survivin mRNA antisense oligonucleotide. When the MUC1 aptamers recognized MUC1 on the cell membrane or the survivin mRNA hybridized with its antisense DNA in the cytoplasm, the fluorescence signals of the corresponding dyes were recovered. This allowed for the simultaneous imaging of MUC1 on the cell membrane and survivin mRNA in the cytoplasm, enabling the visualization of biomarkers with distinct spatial distributions in living cells. To enhance the interplay between COF NPs and functional nucleic acids, a freezing method was proposed to increase the DNA loading density and ensure high detection efficacy. The resultant BOF-based nanoprobe has been further applied to trace biomarkers delivered by bio-vehicles such as exosomes from cancer cells, which could accurately mark cancer cells from normal cells by simultaneously imaging multiple biomarkers. This work broadened the application of BOFs and opened a new door for the rational design of BOF-based nanoprobe for bioanalysis.

## 4 Conclusions and prospects

This review has concisely but comprehensively introduced the synthesis strategies and broad applications of BOFs achieved in recent years, which is expected to be beneficial for readers to catch a fast sight of the state-of-the-art. Although substantial in progress, the proposed research topic is still in a nascent development stage and many challenges need to be addressed in the future.

(1) Biomolecules immobilized through surface attachment always suffer from serious leaching and susceptibility during recycled usage caused by weak interactions between biomolecules and organic frameworks. In contrast, biomolecules installed by pore encapsulation can show greatly improved recycling performances and stabilities. However, only biomolecules that match the pore size of organic frameworks are applicable in principle. In addition, harsh reaction conditions such as high temperatures and nonaqueous solvents required by the syntheses of MOFs and COFs are incompatible with the biomolecules during *in situ* encapsulation. Fortunately, the HOFs that have recently emerged are constructed from moderately linked H-bonds with the unique advantages of facile preparation and dynamic regeneration. Thus, biomolecules are anticipated to be facily embedded within the matrixes of HOFs accompanied by high loading amounts.<sup>91,92</sup>

(2) Due to the low symmetry and high flexibility of biomolecules, it is still challenging to synthesize BOFs with good crystallinity and robust porosity at the same time using biomolecular linkers directly. Distinct from most framework materials that are built from polydentate zero-dimensional (0D) nodes and rigid linkers, the development of frameworks composed of one-dimensional (1D) chain-like or two-dimensional (2D) square-like nodes as unique inorganic pillars might be applicable for matching flexible biomolecules. In particular, with judicious selection of low toxicity compounds, such as alkali and alkali earth metal-oxo nodes as infinite secondary units, the resultant BOFs are expected to be ideal candidates for drug cargo, biosensing, bioimaging and theranostic bio-platforms.

(3) Although some studies have clarified the low toxicity of certain BOFs, real biocompatibility, such as blood compatibility, neurotoxicity, and histocompatibility still need to be systematically explored. As a novel type of biomaterial, for example, BOFs in nano-dimensions may induce unexpected neurotoxicity as they could cross the brain-blood barrier and invade the central nervous system. Moreover, the reported toxicity experiments of BOFs were primarily conducted *in vitro* and needed to be further justified *in vivo*, let alone practical applications at the clinical stage. Definitely, it is a rarely touched land yet awaiting much more efforts devoted to the systematic evaluation of the metabolic outcomes of novel BOF biomaterials.

(4) Apart from the intrinsic properties inherited from parent organic frameworks and/or biomolecules, additional enhancement and even synergistic effects are hoped to appear for intergraded BOFs. However, the rational design and full exploitation of synergy are still far from satisfactory on account of the rarely understood interactions between biomolecules and frameworks. Advanced characterization techniques such as *in situ* microscopic imaging and real-time spectroscopic techniques are powerful techniques indispensable for systematic interaction investigations. In addition, an artificial intelligence-assisted theoretical algorithm that is able to deal with multi-component systems deserves to be fully developed for mechanism understanding.<sup>93,94</sup>

With continuous research efforts, we will see flourishing prospects of applying BOFs and BOF-based composites in more research fields.

## Author contributions

J. G. and M. T. Z. proposed the topic of this review. J. L. and C. Y. L. drafted the raw manuscript, Z. L. Z., Y. X. G., H. L. C. and P. L. discussed and organized the manuscript. J. L. and J. G. co-revised the manuscript.

## Conflicts of interest

There are no conflicts to declare.

## Acknowledgements

This work is supported by the National Natural Science Foundation of China (No. 22103055, 21905195 and 22205159), the National College Students' Innovation and Entrepreneurship Training Program (No. 202210058019), the Science and Technology Plans of Tianjin (No. 21ZYJJC00050 and 22ZYJDS00070), the Natural Science Foundation of Tianjin City (No. 20JCYBJC00800), the PEIYANG Young Scholars Program of Tianjin University (No. 2020XRX-0023), and the Wenzhou Key Laboratory of Biomaterials and Engineering (No. WIUCASSWCL21005).

## References

- 1 K. E. Sapsford, W. R. Algar, L. Berti, K. B. Gemmill, B. J. Casey, E. Oh, M. H. Stewart and Igor L. Medintz, *Chem. Rev.*, 2013, **113**, 1904–2074.
- 2 S. Rana, Y. C. Yeh and V. M. Rotello, *Curr. Opin. Chem. Biol.*, 2010, **14**, 828–834.
- 3 B. Y. S. Kim, J. T. Rutka and W. C. W. Chan, *N. Engl. J. Med.*, 2010, **363**, 2434–2443.
- 4 C. D. Flynn, D. Chang, A. Mahmud, H. Yousefi, J. Das, K. T. Riordan, E. H. Sargent and S. O. Kelley, *Nat. Rev. Bioeng.*, 2023, **1**, 560–575.
- 5 A. Niroula, T. D. Gamot, C. W. Ooi and S. Dhital, *Food Hydrocolloids*, 2021, **112**, 106303.
- 6 Y. R. Maghraby, R. M. El-Shabasy, A. H. Ibrahim and H. M. E. Azzazy, *ACS Omega*, 2023, **8**, 5184–5196.
- 7 B. S. Chhikara and K. Parang, *Chem. Biol. Lett.*, 2023, **1**, 451.
- 8 K. Bhakuni, M. Bisht, P. Venkatesu and D. Monda, *Chem. Commun.*, 2019, **55**, 5747–5750.
- 9 B. Yang, B. N. Zhou, C. F. Li, X. W. Li, Z. W. Shi, Y. X. Li, C. Y. Zhu, X. Li, Y. Hua, Y. F. Pan, J. He, T. Y. Cao, Y. W. Sun, W. L. Liu, M. Ge, Y. H. R. Yang, Y. C. Dong and D. S. Liu, *Angew. Chem., Int. Ed.*, 2022, **61**, e202202520.
- 10 Y. Z. Zhang, J. Tu, D. Q. Wang, H. T. Zhu, S. K. Maity, X. M. Qu, B. Bogaert, H. Pei and H. B. Zhang, *Adv. Mater.*, 2018, **30**, 1703658.
- 11 F. F. Xia, A. X. He, H. T. Zhao, Y. Sun, Q. Duan, S. J. Abbas, J. J. Liu, Z. Y. Xiao and W. H. Tan, *ACS Nano*, 2022, **16**, 169–179.
- 12 S. H. Zhang, W. Xia, Q. Yang, Y. Kaneti, X. T. Xu, S. M. Alshehri, T. Ahamad, Md. S. A. Hossain, J. Na, J. Tang and Y. Yamauchi, *Chem. Eng. J.*, 2020, **396**, 125154.
- 13 J. Guo, Y. Wan, Y. F. Zhu, M. T. Zhao and Z. Y. Tang, *Nano Res.*, 2021, **14**, 2037–2052.
- 14 D. S. Zhen, C. L. Liu, Q. H. Deng, S. Q. Zhang, N. M. Yuan, L. Li and Y. Liu, *Chin. Chem. Lett.*, 2023, 27109249.
- 15 P. G. Qin, S. P. Zhu, M. Y. Mu, Y. M. Gao, Z. W. Cai and M. H. Lu, *Chin. Chem. Lett.*, 2023, **34**, 108620.
- 16 J. Guo, Y. Qin, Y. Zhu, X. Zhang, C. Long, M. Zhao and Z. Tang, *Chem. Soc. Rev.*, 2021, **50**, 5366.
- 17 J. Guo, F. F. Li and Y. Liu, *Matter*, 2021, **4**, 3792–3794.
- 18 S. H. Zhang, Q. Yang, C. Wang, X. L. Luo, J. Kim, Z. Wang and Y. Yamauchi, *Adv. Sci.*, 2018, **5**, 1801116.
- 19 Y. F. Tong, Z. P. Sun, J. W. Wang, W. W. Huang and Q. C. Zhang, *SmartMat*, 2022, **3**, 685–694.
- 20 B. J. Zhang, J. Y. Chen, Z. Zhu, X. Zhang and J. Wang, *Small*, 2023, 2307299.
- 21 F. R. Sha, H. M. Xie, F. A. Son, K. S. Kim, W. Gong, S. Y. Su, K. K. Ma, X. L. Wang, X. J. Wang and O. K. Farha, *J. Am. Chem. Soc.*, 2023, **145**, 16383–16390.
- 22 X. Li, Y. Zhang, W. L. Tan, P. Jin, P. Zhang and K. Li, *Anal. Chem.*, 2023, **95**, 2865–2873.
- 23 M. C. Lv, M. Sun, M. C. Wu, F. Zhang, H. Y. Yin, Y. Sun, R. Liu, Z. Fan and J. Z. Du, *Nano Lett.*, 2022, **22**, 9621–9629.
- 24 Y. T. Li, K. Zhang, P. Liu, M. Chen, Y. L. Zhong, Q. S. Ye, M. Q. Wei, H. J. Zhao and Z. Y. Tang, *Adv. Mater.*, 2019, **31**, 1901570.
- 25 S. Banerjee, C. T. Lollar, Z. Xiao, Y. u. Fang and H.-C. Zhou, *Trends Chem.*, 2020, **2**, 467–479.
- 26 D. Wang, H. Wu, J. Zhou, P. Xu, C. Wang, R. Shi, H. Wang, H. Wang, Z. Guo and Q. Chen, *Adv. Sci.*, 2018, **5**, 1800287.
- 27 C. N. Jin, N. Li, E. Lin, X. P. Chen, T. Wang, Y. Wang, M. F. Yang, W. S. Liu, J. Y. Yu, Z. J. Zhang and Y. Chen, *ACS Catal.*, 2022, **12**, 8259–8268.
- 28 R. Santucci, F. Sinibaldi, P. Cozza, F. Polticelli and L. Fiorucci, *Int. J. Biol. Macromol.*, 2019, **136**, 1237–1246.
- 29 Y. J. Chen, F. Jiménez-Ángeles, B. F. Qiao, M. D. Krzyaniak, F. Sha, S. Kato, X. Y. Gong, C. T. Buru, Z. J. Chen, X. Zhang, N. C. Gianneschi, M. R. Wasielewski, M. O. de la Cruz and O. K. Farha, *J. Am. Chem. Soc.*, 2020, **142**, 18576–18582.
- 30 G. S. Chen, L. J. Tong, S. M. Huang, S. Y. Huang, F. Zhu and G. F. Ouyang, *Nat. Commun.*, 2022, **13**, 4816.
- 31 J. S. Kahn, L. Freage, N. Enkin, M. A. Garcia and I. Willner, *Adv. Mater.*, 2017, **29**, 1602782.
- 32 P. H. Ling, J. P. Lei and H. X. Ju, *Biosens. Bioelectron.*, 2015, **71**, 373–379.
- 33 G. R. Li, Y. J. Wu, C. Zhong, Y. X. Yang and Z. Lin, *Chin. Chem. Lett.*, 2023, 108904.



- 34 Y. Li, W. Ling, X. Y. Liu, X. Shang, P. Zhou, Z. R. Chen, H. Xu and X. Huang, *Nano Res.*, 2021, **14**, 2981–3009.
- 35 W. Gong, Z. J. Chen, J. Q. Dong, Y. Liu and Y. Cui, *Chem. Rev.*, 2022, **122**, 9078–9144.
- 36 Y. L. Zheng, S. N. Zhang, J. B. Guo, R. X. Shi, J. Y. Yu, K. P. Li, N. Li, Z. J. Zhang and Y. Chen, *Angew. Chem., Int. Ed.*, 2022, **61**, e202208744.
- 37 J. Zhuang, A. P. Young and C. K. Tsung, *Small*, 2017, **13**, 1700880.
- 38 X. Z. Lian, Y. Fang, E. Joseph, Q. Wang, J. L. Li, S. Banerjee, C. Lollar, X. Wang and H. C. Zhou, *Chem. Soc. Rev.*, 2017, **46**, 3386–3401.
- 39 D. Q. Chen, D. Z. Yang, C. A. Dougherty, W. F. Lu, H. W. Wu and X. R. He, *ACS Nano*, 2017, **11**, 4315–4327.
- 40 S. Qiao, W. J. Duan, J. Y. Yu, Y. L. Zheng, D. Yan, F. Z. Jin and S. N. Zhang, *ACS Appl. Mater. Interfaces*, 2021, **13**, 32058–32066.
- 41 J. Y. Lu, M. H. Wang, Y. W. Han, Y. Deng, Y. J. Zeng, C. Li, J. Yang and G. X. Li, *Anal. Chem.*, 2022, **94**, 5055–5061.
- 42 T. T. Huo, Y. F. Yang, M. Qian, H. L. Jiang, Y. L. Du, X. Y. Zhang, Y. B. Xie and R. Q. Huang, *Biomaterials*, 2020, **260**, 120305.
- 43 Q. Ye, S. H. Chen, Y. Zhang, B. Ruan, Y. J. Zhang, X. K. Zhang, T. Jiang, X. G. Wang, N. Ma and F. C. Tsai, *Macromol. Biosci.*, 2021, **21**, 2100317.
- 44 C. C. Huang, C. Q. Zhao, Q. Q. Deng, H. C. Zhang, D. Q. Yu, J. S. Ren and X. G. Qu, *Nat. Catal.*, 2023, **6**, 729–739.
- 45 P. Wied, F. Carraro, J. M. Bolivar, C. J. Doonan, P. Falcaro and B. Nidetzky, *Angew. Chem., Int. Ed.*, 2022, **61**, e202117345.
- 46 W. B. Liang, P. Wied, F. Carraro, C. J. Sumby, B. Nidetzky, C. K. Tsung, P. Falcaro and C. J. Doonan, *Chem. Rev.*, 2021, **121**, 1077–1129.
- 47 J. C. Díaz, B. Lozano-Torres and M. Giménez-Marqués, *Chem. Mater.*, 2022, **34**, 7817–7827.
- 48 P. Li, J. A. Modica, A. J. Howarth, E. Vargas, P. Z. Moghadam, R. Q. Snurr, M. Mrksich, J. T. Hupp and O. K. Farha, *Chem*, 2016, **1**, 154–169.
- 49 Q. Sun, B. Aguila, P. C. Lan and S. Ma, *Adv. Mater.*, 2019, **31**, 1900008.
- 50 W. Liang, F. Carraro, M. B. Solomon, S. G. Bell, H. Amenitsch, C. J. Sumby, N. G. White, P. Falcaro and C. J. Doonan, *J. Am. Chem. Soc.*, 2019, **141**, 14298–14305.
- 51 W. Q. Xu, Y. Wu, L. Jiao, M. Sha, X. L. Cai, Y. T. Wen, Y. F. Chen, W. L. Gu and C. Z. Zhu, *Nano Res.*, 2022, **16**, 3364–3371.
- 52 G. S. Chen, S. M. Huang, X. X. Kou, F. Zhu and G. F. Ouyang, *Angew. Chem.*, 2020, **132**, 14051–14058.
- 53 W. Liang, H. Xu, F. Carraro, N. K. Maddigan, Q. Li, S. G. Bell, D. M. Huang, A. Tarzia, M. B. Solomon, H. Amenitsch, L. Vaccari, C. J. Sumby, P. Falcaro and C. J. Doonan, *J. Am. Chem. Soc.*, 2019, **141**, 2348–2355.
- 54 F. S. Liao, W. S. Lo, Y. S. Hsu, C. C. Wu, S. C. Wang, F. K. Shieh, J. V. Morabito, L. Y. Chou, K. C. W. Wu and C. K. Tsung, *J. Am. Chem. Soc.*, 2017, **139**, 6530–6533.
- 55 D. Q. Yu, H. C. Zhang, Z. Q. Liu, C. Liu, X. B. Du, J. S. Ren and X. G. Qu, *Angew. Chem.*, 2022, **134**, e202201485.
- 56 X. C. Jiang, J. J. Xiang, H. H. Wu, T. Y. Zhang, D. P. Zhang, Q. H. Xu, X. L. Huang, X. L. Kong, J. H. Sun, Y. L. Hu, K. Li, Y. Tabata, Y. Q. Shen and J. Q. Gao, *Adv. Mater.*, 2019, **31**, 1807591.
- 57 D. H. Huang, Y. H. Cao, X. Yang, Y. Y. Liu, Y. J. Zhang, C. Y. Li, G. C. Chen and Q. B. Wang, *Adv. Mater.*, 2021, **33**, 2006357.
- 58 Y. Feng, X. Cao, L. Zhang, J. Y. Li, S. T. Cui, Y. X. Bai, K. Q. Chen and J. Ge, *Chem. Eng. J.*, 2022, **439**, 135736.
- 59 S. J. Wang, M. Wahiduzzaman, L. Davis, A. Tissot, W. Shepard, J. Marrot, C. Martineau-Corcus, D. Hamdane, G. Maurin, S. Devautour-Vinot and C. Serre, *Nat. Commun.*, 2018, **9**, 4937.
- 60 M. Mon, R. Bruno, R. Lappano, M. Maggolini, L. D. Donna, J. F. Soria, D. Armentano and E. Pardo, *Inorg. Chem.*, 2021, **60**, 14221–14229.
- 61 R. Chen, Z. X. Yao, N. Han, X. C. Ma, L. Q. Li, S. Liu, H. Q. Sun and S. Wang, *ACS Omega*, 2020, **5**, 15402–15408.
- 62 S. L. Anderson, P. G. Boyd, A. Gladysiak, T. N. Nguyen, R. G. Palgrave, D. Kubicki, L. Emsley, D. Bradshaw, M. J. Rosseinsky, B. Smit and K. C. Stylianou, *Nat. Commun.*, 2019, **10**, 1612.
- 63 A. Sorrenti, L. Jones, S. Sevim, X. B. Cao, A. J. deMello, C. Marti-Gastaldo and J. Puigmartí-Luis, *J. Am. Chem. Soc.*, 2020, **142**, 9372–9381.
- 64 P. A. Sontz, J. B. Bailey, S. Ahn and F. A. Tezcan, *J. Am. Chem. Soc.*, 2015, **137**, 11598–11601.
- 65 W. Maret and Y. Li, *Chem. Rev.*, 2009, **109**, 4682–4707.
- 66 G. S. Chen, S. M. Huang, X. X. Kou, X. M. Ma, S. Y. Huang, Q. Tong, K. L. Ma, W. Chen, P. Y. Wang, J. Shen, F. Zhu and G. F. Ouyang, *Chem*, 2021, **7**, 2722–2742.
- 67 H. Musarurwa and N. T. Tavengwa, *Carbohydr. Polym.*, 2022, **275**, 118743.
- 68 B. Zhang, H. W. Chen, Q. H. Hu, L. M. Jiang, Y. Q. Shen, D. Zhao and Z. X. Zhou, *Adv. Funct. Mater.*, 2021, **31**, 2105395.
- 69 S. Dutta, *Adv. NanoBiomed Res.*, 2020, **1**, 2000010.
- 70 H. Li, Y. W. Zhang, Y., C. Zhang, F. X. Wei, Y. F. Deng, Z. H. Lin, C. H. Xu, L. H. Fu and B. F. Lin, *Carbohydr. Polym.*, 2023, **301**, 120317.
- 71 K. J. Hartlieb, J. M. Holcroft, P. Z. Moghadam, N. A. Vermeulen, M. M. Algaradah, M. S. Nassar, Y. Y. Botros, R. Q. Snurr and J. F. Stoddart, *J. Am. Chem. Soc.*, 2016, **138**, 2292–2301.
- 72 D. Shen, J. A. Cooper, P. Li, Q. H. Guo, K. Cai, X. J. Wang, H. Wu, H. L. Chen, L. Zhang, Y. Jiao, Y. Qiu, C. L. Stern, Z. Liu, A. C.-H. Sue, Y.-W. Yang, F. M. Alsubaie, O. K. Farha and J. F. Stoddart, *J. Am. Chem. Soc.*, 2020, **142**, 2042–2050.
- 73 G. X. Lan, Y. J. Fan, W. J. Shi, E. You, S. S. Veroneau and W. B. Lin, *Nat. Catal.*, 2022, **5**, 1006–1018.
- 74 Y. X. Guo, Q. Sun, F. G. Wu, Y. L. Dai and X. Y. Chen, *Adv. Mater.*, 2021, **33**, 2007356.
- 75 G. W. Chong, J. Zang, Y. Han, R. P. Su, N. Weeranoppanan, H. Q. Dong and Y. Y. Li, *Nano Res.*, 2021, **14**, 1244–1259.

- 76 G. Y. Zhang, X. L. Li, Q. B. Liao, Y. F. Liu, K. Xi, W. Y. Huang and X. D. Jia, *Nat. Commun.*, 2018, **9**, 2785.
- 77 C. Liu, B. Liu, J. Zhao, Z. H. Di, D. Q. Chen, Z. J. Gu, L. L. Li and Y. L. Zhao, *Angew. Chem., Int. Ed.*, 2020, **59**, 2634–2638.
- 78 J. T. Liu, B. J. C. Wong, T. R. Liu, H. Yang, L. Y. Ye and J. P. Lei, *Chem. – Eur. J.*, 2022, **28**, e202200305.
- 79 H. Xia, N. Li, W. Q. Huang, Y. Song and Y. B. Jiang, *ACS Appl. Mater. Interfaces*, 2021, **13**, 22240–22253.
- 80 Y. J. Chen, P. Li, H. Noh, C. W. Kung, C. T. Buru, X. J. Wang, X. Zhang and O. K. Farha, *Angew. Chem., Int. Ed.*, 2019, **58**, 7682–7686.
- 81 R. Newar, N. Akhtar, N. Antil, A. Kumar, S. Shukla, W. Begum and K. Manna, *Angew. Chem., Int. Ed.*, 2021, **60**, 10964–10970.
- 82 J. Navarro-Sánchez, A. I. Argente-García, Y. Moliner-Martínez, D. Roca-Sanjuán, D. Antypov, P. Campins-Falcó, M. J. Rosseinsky and Carlos Marti-Gastaldo, *J. Am. Chem. Soc.*, 2017, **139**, 4294–4297.
- 83 S. N. Zhang, Y. L. Zheng, H. D. An, B. Aguila, C. X. Yang, Y. Y. Dong, W. Xie, P. Cheng, Z. J. Zhang, Y. Chen and S. Q. Ma, *Angew. Chem., Int. Ed.*, 2018, **57**, 16754–16759.
- 84 Y. Yan, E. J. Carrington, R. Pétuya, G. F. S. Whitehead, A. Verma, R. K. Hylton, C. C. Tang, N. G. Berry, G. R. Darling, M. S. Dyer, D. Antypov, A. P. Katsoulidis and M. J. Rosseinsky, *J. Am. Chem. Soc.*, 2020, **142**, 14903–14913.
- 85 X. H. Zheng, L. Wang, M. Liu, P. P. Lei, F. Liu and Z. G. Xie, *Chem. Mater.*, 2018, **30**, 6867–6876.
- 86 Y. F. Zhao, H. Zeng, X. W. Zhu, W. G. Lu and D. L., *Chem. Soc. Rev.*, 2021, **50**, 4484–4513.
- 87 X. X. Mao, F. N. He, D. H. Qiu, S. J. Wei, R. G. Luo, Y. Chen, X. B. Zhang, J. P. Lei, D. Monchaud, J. Mergny, H. X. Ju and J. Zhou, *Anal. Chem.*, 2022, **94**, 7295–7302.
- 88 X. L. Dou, G. Wu, Z. Y. Ding and J. Xie, *Food Chem.*, 2023, **416**, 135805.
- 89 H. M. Meng, X. X. Shi, J. Chen, Y. H. Gao, L. B. Qu, K. Zhang, X. B. Zhang and Z. H. Li, *ACS Sens.*, 2020, **5**, 103–109.
- 90 P. Gao, R. Y. Wei, Y. Y. Chen, X. H. Liu, J. Zhang, W. Pan, N. Li and B. Tang, *Anal. Chem.*, 2021, **93**, 13734–13741.
- 91 Y. D. Shi, S. D. Wang, W. Tao, J. J. Guo, S. Xie, Y. L. Ding, G. Y. Xu, C. Chen, X. Y. Sun, Z. M. Zhang, Z. K. He, P. F. Wei and B. Z. Tang, *Nat. Commun.*, 2022, **13**, 1882.
- 92 H. Yamagishi, H. Sato, A. Hori, Y. Sato, R. Matsuda, K. Kato and T. Aida, *Science*, 2018, **361**, 1242–1246.
- 93 B. Burge, P. M. Maffettone, V. V. Gusev, C. M. Aitchison, Y. Bai, X. Y. Wang, X. B. Li, B. M. Alston, B. Y. Li, R. Clowes, N. Rankin, B. Harris, R. S. Sprick and A. I. Cooper, *Nature*, 2020, **583**, 237–241.
- 94 J. Khan, R. T. M. Ahmad, J. Y. Tan, R. J. Zhang, U. Khan and B. L. Liu, *SmartMat*, 2023, **4**, e1156.
- 95 W. L. Teo, J. W. Liu, W. Q. Zhou and Y. L. Zhao, *SmartMat*, 2021, **2**, 567–578.
- 96 F. F. Li, Y. L. Duan, J. Li, X. M. Xue, Y. X. Guo, Y. L., Z. J. Yang, X. F. Zhang and J. Guo, *TrAC, Trends Anal. Chem.*, 2024, **170**, 117471.